

# **REAL-TIME TWO-WAY TIME TRANSFER TO AIRCRAFT**

**Jeremy Warriner, Symmetricom**

**Capt. Richard Beckman, USAF**

**Tom Celano, Symmetricom**

**Mikel Miller and Peter Howe**

**U.S. Air Force Research Laboratory**

## **Abstract**

*Two-way time transfer (TWTT) has proven itself as an accurate and reliable method for synchronization over large static baselines. While previous demonstrations have shown the merit of extending TWTT to dynamic platforms, the technology has always been dogged by the fact that it requires specialized equipment and post-processing of the data. If TWTT is to establish itself as a viable means of synchronization between dynamic platforms, it must first demonstrate the ability to operate in real-time with COTS hardware. The most recent airborne test set out to demonstrate this capability and the results of that test are presented herein.*

## **1.0 INTRODUCTION**

Although TWTT has become the standard for precise time synchronization across large baselines, it has yet to make the leap to synchronization of dynamic platforms in an operational context. This is due largely to the additional processing burden required to correct TWTT measurements from dynamic platforms and in part to the additional complexity involved in calibrating dynamic platforms. Previous work has shown the capability of TWTT techniques to be extended to the dynamic case with accuracies superior to those obtainable with current GPS techniques [1]. However, TWTT to a dynamic platform has never been performed in real time and has, thus, remained unutilized as a method for inter-platform synchronization.

This work extends the TWTT concepts to a real-time implementation of a dynamic scenario. Furthermore, the concepts are validated experimentally using COTS equipment and serve as an example of the accuracies obtainable with dynamic TWTT. This results in a new capability for users that either need performance better than can be provided by GPS or need an alternative to GPS.

## 2.0 PRINCIPLES OF TWTT

### STATIC TWTT

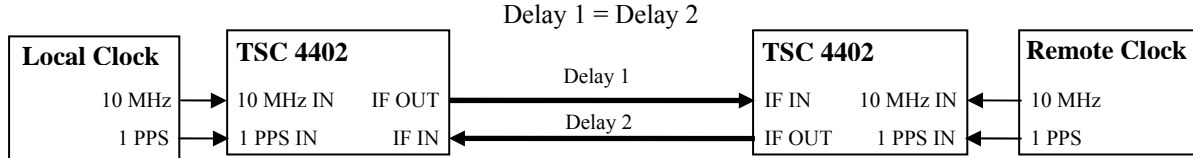


Figure 1. Setup for static TWTT.

Static TWTT is not explored in exhaustive detail here because numerous articles have been written on the topic [2,3]. The basic premise of the technique is summed up in Figure 1, which uses a time transfer modem (TSC 4402) to generate a time-based waveform coherent with the timing signals provided by the clock. The time transfer modem then measures the relative time between when the signal was transmitted and when the signal from the opposite side was received. The offset between the two clocks can then be determined using Equation 1.

$$\text{RemoteClockDelay} = \frac{(\text{MEAS}_{\text{Remote}} - \text{MEAS}_{\text{Local}})}{2} \quad (1)$$

where:

- $\text{MEAS}_{\text{Remote}}$  = TSC 4402 measurement made by the remote system
- $\text{MEAS}_{\text{Local}}$  = TSC 4402 measurement made by the local system.

Although the calculation in Equation 1 is trivial, it is important to recognize the following two constraints before solving a TWTT problem:

1. The time at which the time-based signal is transmitted is the same for both sides.
2. The propagation delay of the transmitted signal must be the same in both directions.

In this case, the first constraint is handled automatically by the time transfer modem, but the burden of complying with the second constraint is left to the user. If both constraints have been met, then the offset between the two clocks can be determined using the standard TWTT equation given in Equation 1.

### Dynamic TWTT

Dynamic TWTT extends the static TWTT principles to moving platforms. The primary difference is that, because one or both of the platforms is moving during the measurement interval, the second constraint of TWTT is not satisfied. Figure 2 shows a typical setup for dynamic TWTT involving an aircraft. In this case, a geosynchronous satellite is being used as the relay and the reader should note that the path traveled by the aircraft's transmitted signal is different than the path traveled by the received signal. Clearly, this violates the constraint that the path delay of both signals be equal. In addition to the obvious correction for the motion of the aircraft, there is an additional correction that must be made due to the fact that the entire TWTT system exists in a noninertial reference frame (i.e., the Earth). This effect is known as the Sagnac effect and is significant due to the large separation between the ground station and the aircraft.

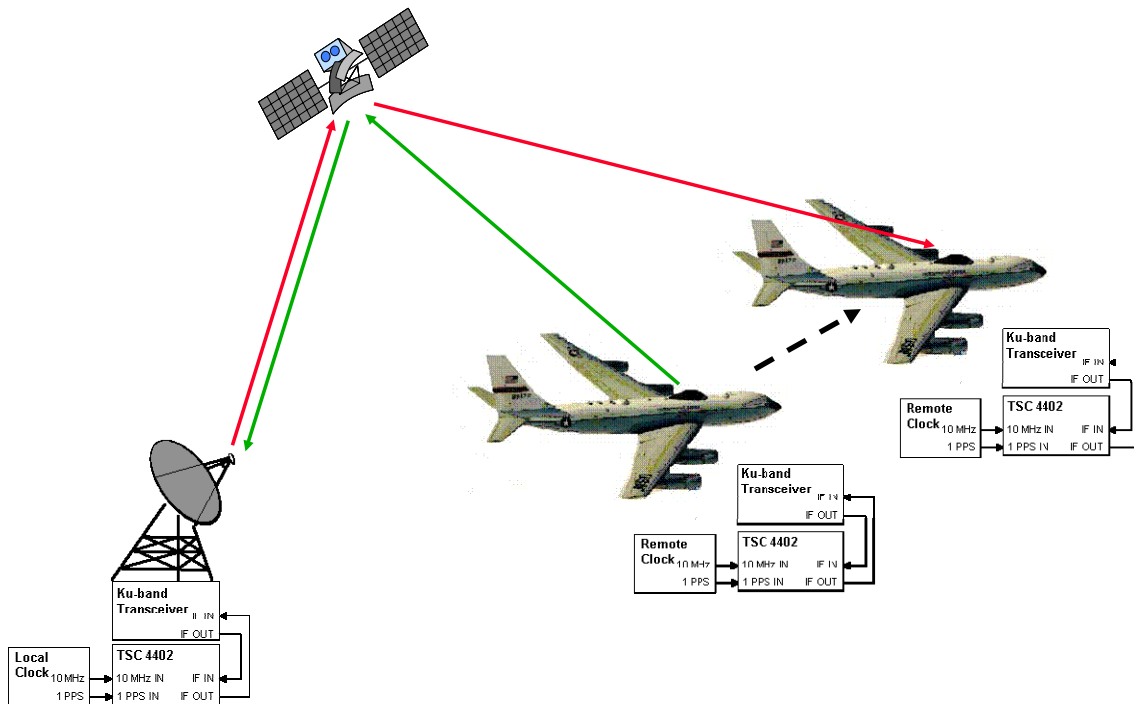


Figure 2. Setup for dynamic TWTT.

Applying corrections to Equation 1 for the two effects just discussed yields the following result.

$$\text{Re } \text{moteClockDelay} = \frac{(\text{MEAS}_{\text{Re } \text{mote}} - \text{MEAS}_{\text{Local}}) + \Delta_{\text{prop\_delay}} + \Delta_{\text{Sagnac}}}{2} \quad (2)$$

where:

- |                               |   |
|-------------------------------|---|
| $\text{MEAS}_{\text{Remote}}$ | = TSC 4402 measurement made by the remote system          |
| $\text{MEAS}_{\text{Local}}$  | = TSC 4402 measurement made by the local system           |
| $\Delta_{\text{prop\_delay}}$ | = difference in propagation delay of the two signal paths |
| $\Delta_{\text{Sagnac}}$      | = difference in the Sagnac effect of the two signal paths |

Experiments conducted in 2002 successfully demonstrated the non-real-time extension of TWTT to the dynamic case in with sub-nanosecond accuracy [1].

### 3.0 REAL-TIME DYNAMIC TWTT

The corrections identified in Equation 2 must be calculated in real time if a viable TWTT system is to be implemented. Traditional methods of calculating the corrections are possible, but require both sides of the link to transmit additional data in order to perform the calculation. These data relate to specifics about the motion of platform, such as position and velocity. To minimize the amount of data required to be transmitted over the link, the TWTT calculation can be expressed in the following form:

$$\text{RemoteClockDelay} = \frac{(\text{Corrected}_{\text{Remote}} - \text{Corrected}_{\text{Local}})}{2} \quad (3)$$

where:

$$\text{Corrected}_{\text{Local}} = \text{MEAS}_{\text{Local}} + \text{MOTION}_{\text{Local}} + \text{SAGNAC}_{\text{Local}} \quad (4)$$

and

$$\text{Corrected}_{\text{Remote}} = \text{MEAS}_{\text{Remote}} + \text{MOTION}_{\text{Remote}} + \text{SAGNAC}_{\text{Remote}}. \quad (5)$$

This scenario requires each side of the link to correct its measurement before relaying that information to the remote system. As a result, the amount of information about the remote platform that must be processed by the local system is reduced. The only step left is to determine the necessary corrections that must be applied to the local measurement.

The first correction applied is identified by the  $\text{MOTION}_{\text{Local}}$  term. It corrects for local platform motion occurring during the measurement interval and is determined using the following equation.

$$\text{MOTION}_{\text{Local}} = \frac{\mathbf{v}_{\text{loc}} \cdot (\mathbf{x}_{\text{rem}} - \mathbf{x}_{\text{loc}})}{\frac{\mathbf{v}_{\text{loc}} \cdot (\mathbf{x}_{\text{rem}} - \mathbf{x}_{\text{loc}})}{c + c^2} + \frac{(\mathbf{v}_{\text{loc}} \cdot (\mathbf{x}_{\text{rem}} - \mathbf{x}_{\text{loc}}))}{c \|\mathbf{x}_{\text{rem}} - \mathbf{x}_{\text{loc}}\|}} \quad (6)$$

where:

- $\mathbf{x}_{\text{loc}}$  = position vector (ECEF datum) of the local platform
- $\mathbf{x}_{\text{rem}}$  = position vector (ECEF datum) of the remote platform
- $\mathbf{v}_{\text{loc}}$  = velocity vector (ECEF datum) of the local platform
- $t_{\text{loc}}$  = time the local timing signal is transmitted
- $t_{\text{rem}}$  = time the remote timing signal is transmitted
- $c$  = speed of light.

The correction given in Equation 6 is comprised of two terms. The first term calculates the change in path delay, assuming that both signals are transmitted simultaneously, and the second term is an additional correction for when the signals are not transmitted simultaneously.

The second correction applied in Equation 4 is a direct result of the Sagnac effect and is given by the following equation:

$$\text{SAGNAC}_{\text{Local}} = \frac{2\omega[(\mathbf{x}_{\text{loc}} \cdot \hat{\mathbf{x}})\hat{\mathbf{x}} + (\mathbf{x}_{\text{loc}} \cdot \hat{\mathbf{y}})\hat{\mathbf{y}}] \times [(\mathbf{x}_{\text{rem}} \cdot \hat{\mathbf{x}})\hat{\mathbf{x}} + (\mathbf{x}_{\text{rem}} \cdot \hat{\mathbf{y}})\hat{\mathbf{y}}] \cdot \hat{\mathbf{z}}}{c^2} \quad (7)$$

where:

- $\mathbf{x}_{\text{loc}}$  = position vector (ECEF datum) of the local platform
- $\mathbf{x}_{\text{rem}}$  = position vector (ECEF datum) of the remote platform
- $c$  = speed of light
- $\omega$  = angular velocity of the Earth.

The nuance of Equations 6 and 7 is that the remote platform refers to the last platform the signal emanated from. Thus, in the case of a satellite relay, the remote platform refers to the satellite and not the remote timing system as one might intuitively guess. Additionally, Equations 6 and 7 only hold true when using a single satellite relay. For a line-of-sight link, the correction in Equation 7 must be halved and RF links that include more than one relay require additional corrections and are not discussed here.

## 4.0 FLIGHT TEST

A flight test was conducted at Kirtland AFB in April 2006 to experimentally validate the equations given in Section 3. For the purpose of determining the measurement accuracy of the system under test, two identical but independent systems operated throughout the experiment. Each system operated over its own dedicated communication link and unique satellite. In this way, both systems are measuring the time difference between the ground clock and the flight clock, but any error in the real-time equations would manifest itself differently in the two links and be readily apparent in the output data.

Prior to the flight, both clocks were co-located at Kirtland AFB and characterized with respect to one other. This served as the basis for the “true” clock offset prior to the flight. Immediately before take-off, the flight clock was transported to the aircraft and served as the time source for both airborne TWTT systems. Following the installation of the flight clock, the RF communication links were established and then each time transfer modem began providing clock offset measurements between the ground clock and the flight clock. After completing the 6-hour flight, the flight clock was returned to the hangar where it was once again compared to the ground clock using a time-interval counter. This measurement serves as the “true” clock offset after the flight.

The experimental setup during the flight is illustrated in Figure 3. As previously stated, two independent systems were operated throughout the flight to measure the offset between the ground clock and the flight clock. The two systems are distinguished by the nomenclature “Side A” and “Side B.”

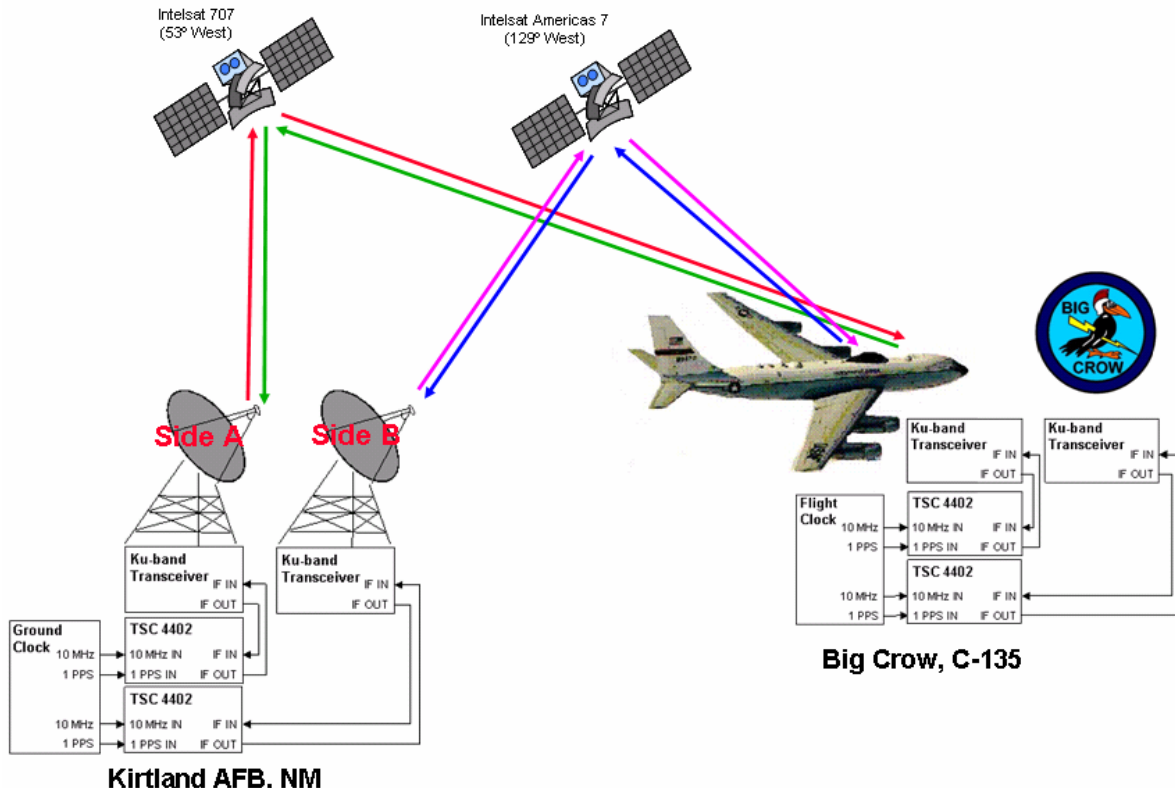


Figure 3. Experimental setup for flight test.

During the flight, a TSC 4400 (GPS Time & Frequency Standard) served as the network time server for the time transfer modem. This was necessary so that the 10 MHz and 1 PPS signals from the flight clock could be properly assigned to the correct second. Additionally, the TSC 4400 provided real-time GPS data to the time transfer modem so that the measurement corrections laid out in Section 3 could be calculated in real time. No other equipment was required to enable the real-time dynamic measurement capability of the time transfer modem.

Figure 4 is a map plot of the flight path taken. The ground clock was located at Kirtland AFB and, thus, the flight originated and ended there so that the flight clock could be immediately transported to the hangar for comparison with the ground clock. The only time the two measurement systems were shut down during the flight was during a 40-minute period in which the aircraft was being refueled in air. This was required to extend the duration of the flight and is shown in Figure 4 as well.

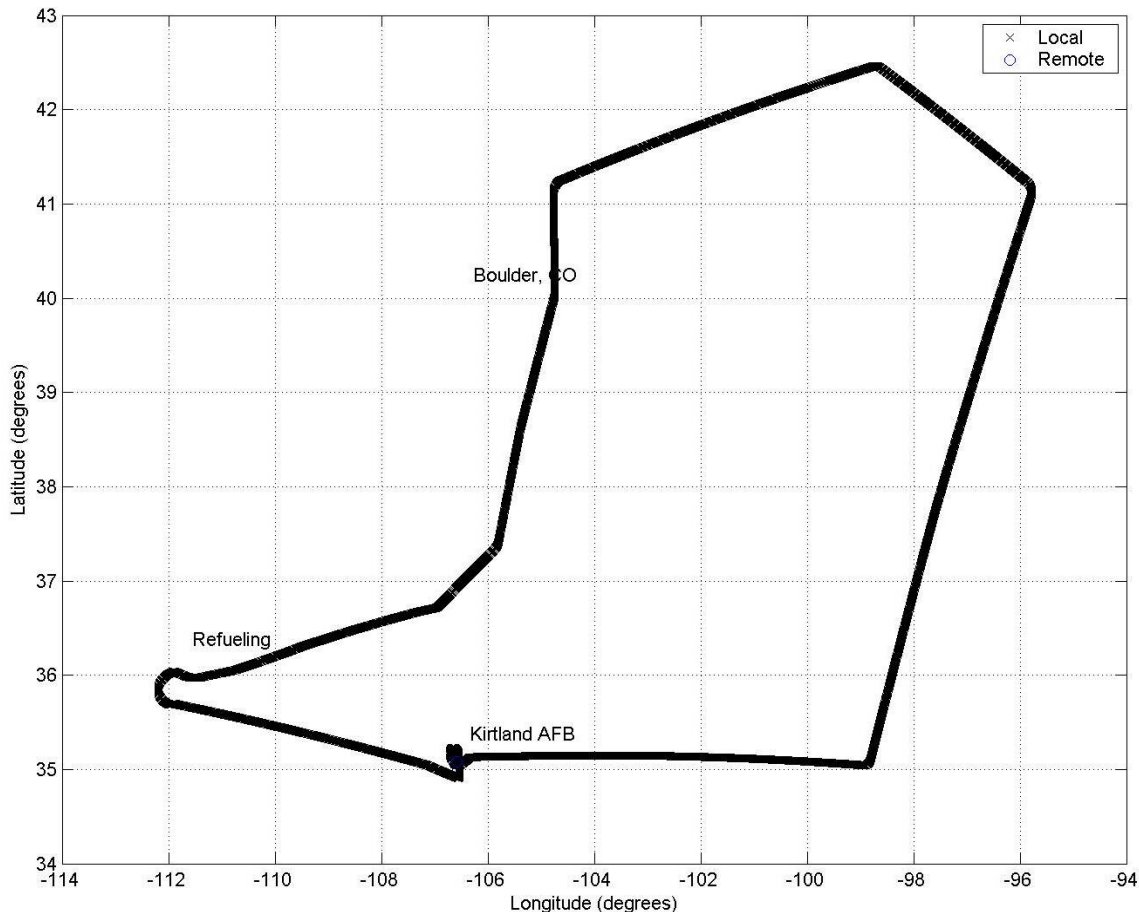


Figure 4. Map plot of the flight path.

Figure 5 displays the uncorrected TWTT measurements during the flight. The dominant effect seen in the plot is correlated to the range rate of the aircraft in the direction of the satellite relay. Because two different satellites are being used, the range rate for the two systems is quite different and, thus, the raw measurements from the two systems are largely uncorrelated.

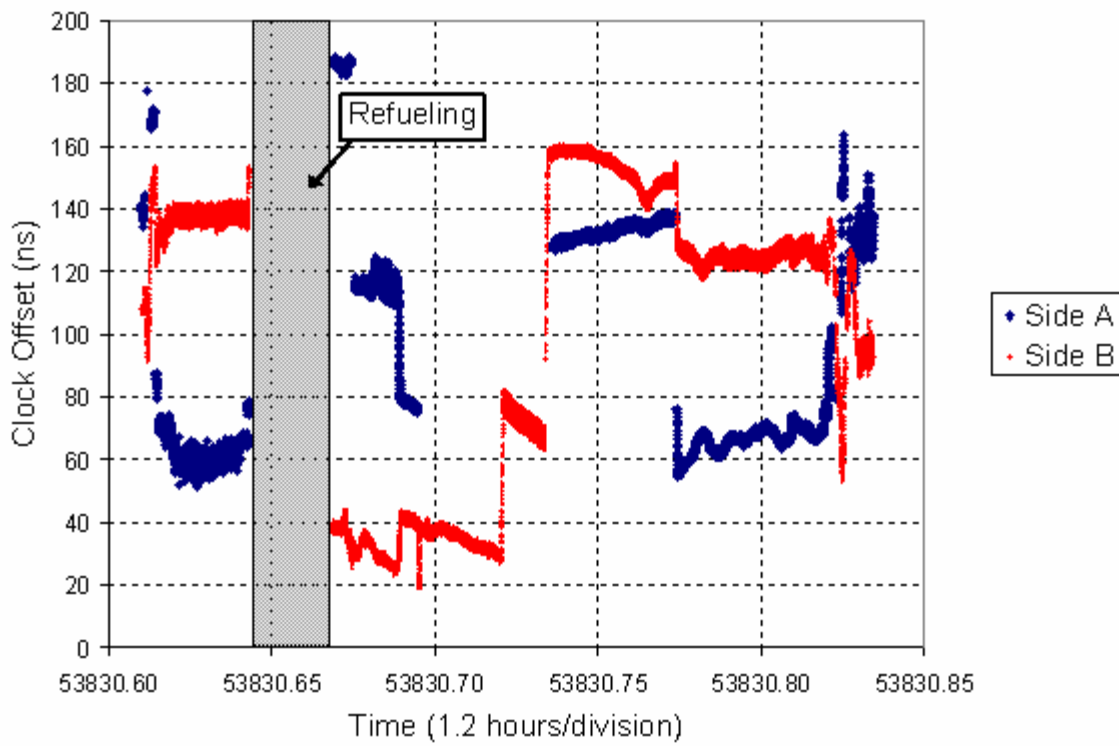


Figure 5. Uncorrected dynamic TWTT measurements.

Applying the real-time corrections to the data yields the plot in Figure 6. The data shown are a 60-second average of the real-time data and are not the real-time output of the time transfer modem. They are averaged only to give a sense of the agreement between the two systems and not to provide a metric for performance. As can be seen from the plot, the agreement between Side A and Side B is very good throughout the course of the flight. Furthermore, the corrected TWTT data agree with the pre-flight and post-flight data shown in blue.

Now that the real-time TWTT equations have been validated against experimental data, the remainder of the data presented will be strictly real-time data in which no averaging occurs. This shall serve as an initial metric for the performance of the time transfer modem and the accuracies obtainable using the TWTT techniques described herein.

Figure 7 compares the data from the two systems during the flight. The primary difference between the data sets is the increased measurement noise of side B with respect to the measurement noise of side A. This is the result of a multi-path scenario that arose due to a second satellite being very near the location of the satellite used for side B. Normal ground stations do not experience this problem, but because of the small aperture size of the aircraft antenna and the errors associated with the antenna tracking algorithm, some energy passes through the adjacent satellite. This signal experiences a different path delay than the primary signal and essentially appears as interference that results in additional measurement noise. Figure 8 is a close-up of the noise on side B resulting from this multi-path scenario.

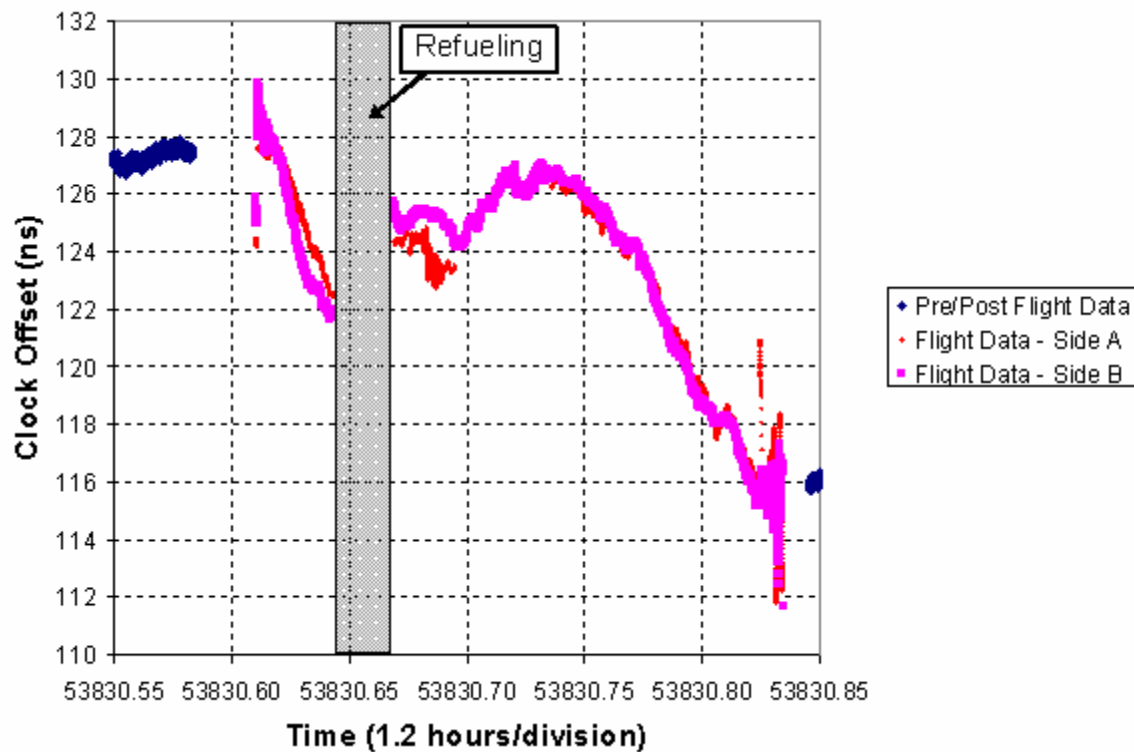


Figure 6. Real-time dynamic TWTT measurements (60-second average).

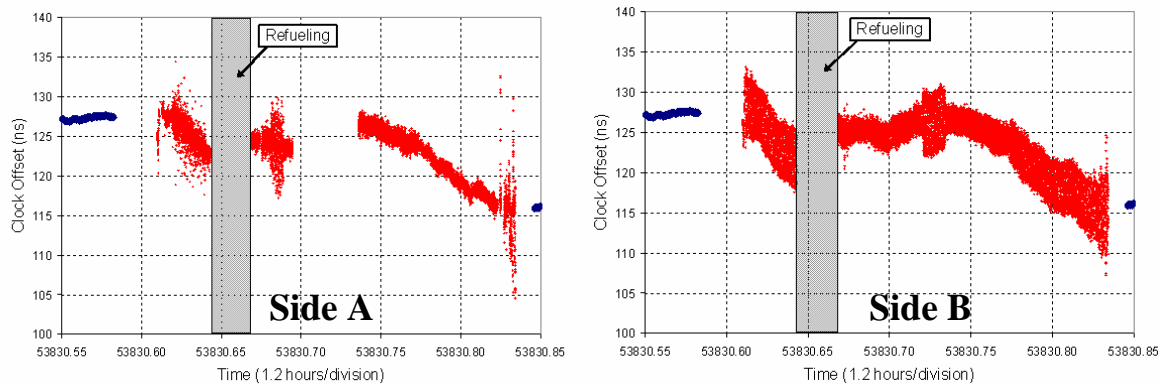


Figure 7. Real-time dynamic TWTT measurements (1-second interval).

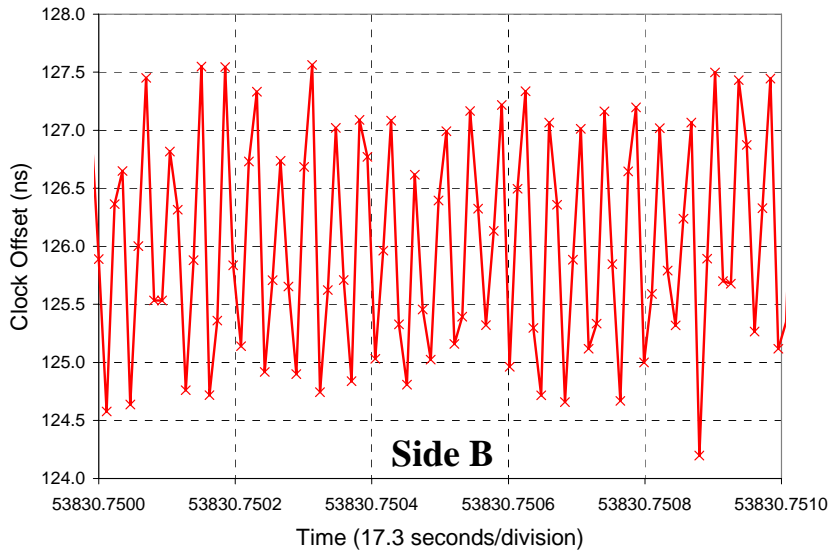


Figure 8. Noise resulting from multi-path scenario on side B.

In addition to the absence of data during aircraft refueling, there is a period on side A when no data was collected. This is the result of insufficient link margin during that portion of the flight. During that period, the signal's pierce point through the antenna radome is in a section that induces greater signal loss than other sections. The additional loss was great enough to prevent the time transfer modem from acquiring the timing signal and making TWTT measurements.

In order to quantify the performance of real-time dynamic TWTT, the data from Side A are trimmed to a 2-hour period in which the RF portion of the system was operating effectively. These data are then compared to the 60-second average from Side B so that its noise does not significantly contribute to the calculation of the residual. The difference between these two data sets serves as the basis for obtaining a metric on the accuracy of the TWTT system. Figure 9 shows the result of this calculation.

## 5.0 CONCLUSIONS

The successful flight demonstration presented here not only validates the extension of TWTT to a real-time dynamic scenario but also validates the concept of using dynamic TWTT in an operational context. The 600 ps accuracy obtained over a 2-hour portion of the flight represents a heretofore inconceivable level of synchronization between platforms. As this is the first demonstration of this technology, its performance will almost certainly improve as the technology matures. This opens the door to numerous military and scientific applications that were previously infeasible due to their stringent cross-platform timing requirements.

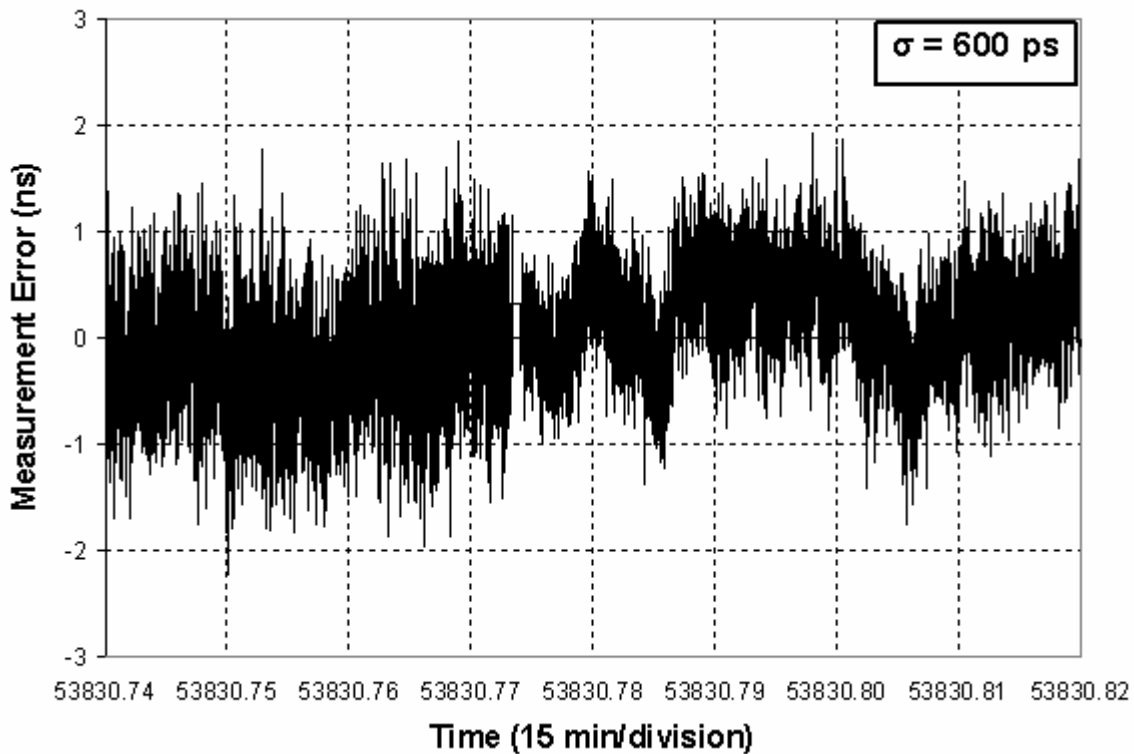


Figure 9. Real-time TWTT performance to an aircraft.

## REFERENCES

- [1] T. Celano, J. Warriner, S. Francis, A. Gifford, P. Howe, and R. Beckman, 2004, “*Two-Way Time Transfer to Airborne Platforms Using Commercial Satellite Modems*,” in Proceedings of the 34<sup>th</sup> Annual Precise Time and Time Interval (PTTI) Systems and Applications Meeting, 3-5 December 2003, Reston, Virginia, USA (U.S. Naval Observatory, Washington, D.C.), pp. 353-366.
- [2] T. Celano, R. Beckman, J. Warriner, S. Francis, A. Gifford, and D. Howe, 2003, “*Dynamic Two-Way Time Transfer to Moving Platforms*,” in Proceedings of the 2003 IEEE International Frequency Control Symposium & PDA Exhibition Jointly with the 17<sup>th</sup> European Frequency and Time Forum (EFTF), 5-8 May 2003, Tampa, Florida, USA (IEEE), pp. 266-272.
- [3] D. W. Hanson, 1989, “*Fundamentals of Two-Way Time Transfers by Satellite*,” in Proceedings of the 43<sup>rd</sup> Annual Frequency Control Symposium, 31 May-2 June 1989, Denver, Colorado, USA (IEEE 89CH2690-6), pp. 174-178.
- [4] T. P. Celano, S. P. Francis, and G. A. Gifford, 2000, “*Continuous Satellite Two-Way Time Transfer Using Commercial Modems*,” in Proceedings of the 2000 IEEE International Frequency Control Symposium, 7-9 June 2000, Kansas City, Missouri, USA (IEEE 00CH37052), pp. 607-611.

- [5] T. P. Celano, S. P. Francis, G. A. Gifford, B. J. Ramsey, and T. L. Erickson, 2001, “*Results of a Continuous Transatlantic Two-Way Satellite Time Transfer Test Using Commercial Modems*,” in Proceedings of the 32<sup>nd</sup> Annual Precise Time and Time Interval (PTTI) Systems and Applications Meeting, 28-30 November 2000, Reston, Virginia, USA (U.S. Naval Observatory, Washington, D.C.), pp. 211-219.
- [6] R. A. Nelson, 2002, **Handbook on Relativistic Time Transfer**.

*38<sup>th</sup> Annual Precise Time and Time Interval (PTTI) Meeting*